

VEGF-mediated tumour growth and EMT in 2D and 3D cell culture models of hepatocellular carcinoma

PREETY RAWAL¹, DINESH MANI TRIPATHI², VIKRANT NAIN¹ and SAVNEET KAUR²

¹School of Biotechnology, Gautam Buddha University, Greater Noida, Uttar Pradesh 201312; ²Department of Molecular and Cellular Medicine, Institute of Liver and Biliary Sciences, New Delhi, Delhi 110070, India

Received February 4, 2022; Accepted May 31, 2022

DOI: 10.3892/ol.2022.13435

Abstract. The purpose of the present study was to evaluate the effects of vascular endothelial growth factor (VEGF) on tumorigenic properties in two-dimensional (2D) and three-dimensional (3D) cultures of hepatoma cells. The proliferation and invasion of hepatoma cells was assessed using wound healing, chemotaxis Transwell, invasion, tube-forming and hanging drop assays in both 2D and 3D cultures. The expression levels of epithelial-mesenchymal transition (EMT) and stemness markers were analysed using reverse transcription-quantitative PCR (RT-qPCR) for mRNA expression and immunofluorescence assay for protein expression. To validate the role of VEGF in tumour growth, a VEGF receptor (VEGFR) inhibitor (sorafenib) was used. The results demonstrated that the hepatoma cells formed 3D spheroids that differed in size and density in the absence and presence of the growth factor, VEGF. In all spheroids, invasion and angiogenesis were more aggressive in 3D cultures in comparison to 2D conditions following treatment with VEGF. Mechanistically, the VEGF-mediated increase in the levels of EMT markers, including Vimentin, N-cadherin 2 (Cadherin 2) and Thy-1 Cell Surface Antigen was observed in the 2D and 3D cultures. Sorafenib treatment for 24 h culminated in a marked reduction in cell migration, cell-cell adhesion, spheroid compaction and EMT gene expression in 3D models as compared to the 2D models. On the whole, the findings of the present study suggested that as compared to the 2D cell cultures, 3D cell cultures model may be used as a more realistic model for the study of tumour growth and invasion in the presence of angiogenic factors, as well as for tumour inhibitor screening.

Introduction

Hepatocellular carcinoma (HCC) is one of the most lethal cancer types worldwide (1). It is a highly vascularized tumour and angiogenesis plays a crucial role in its development, invasion and metastasis. The induction of angiogenesis has been recognized as a crucial step for HCC progression and one of the hallmarks of HCC progression (2-5). The process of angiogenesis comprises of an active proliferation and new vessel formation of vascular endothelial cells, followed by the release of several growth factors, including vascular endothelial growth factor (VEGF), platelet-derived growth factor and erythropoietin (6-8). One of the main associations between angiogenesis and HCC growth is the transition of epithelial liver cells to a mesenchymal phenotype, specified as epithelial-mesenchymal transition (EMT) by angiogenic growth factors, such as VEGF (9-12). EMT confers traits of mesenchymal cells to hepatic tumour cells, which subsequently display a high motility and aggressiveness. Thus, tumour cells acquire the ability to easily enter the bloodstream by invading tumour tissues and blood vessel walls, ultimately resulting in metastasis (8). Hepatic tumour growth, angiogenesis and EMT have been mostly studied in two-dimensional (2D) cell line models *in vitro*; however, they may not be the ideal system for the elucidation of the underlying molecular mechanisms as they do not mimic the complex *in vivo* tumour tissue architecture. It has been reported in recent studies that three dimensional (3D) models more closely resemble the *in vivo* tumour microenvironment by exhibiting complex phenotypic heterogeneity. It has been illustrated that cell-matrix interactions are better recreated by complex aggregated cell populations in 3D culture systems rather than simple 2D cell monolayers (13,14). 3D *in vitro* models of HCC recapitulate the phenotypic and functional characteristics of the *in vivo* liver tissue and hence may be best suited to comprehend the role of growth factors in inducing EMT and tumour growth (15,16). VEGF is one of the key cytokines that affects tumour survival, spread and aggressiveness. The effect of VEGF has been evaluated on several tumour cell lines using conventional two-dimensional (2D) cell culture models; however, they have provided only limited information. Provided that three-dimensional (3D) cell spheroid cultures closely mimic the *in vivo*-like microenvironments, the effects of exogenous treatment with

Correspondence to: Dr Savneet Kaur, Department of Molecular and Cellular Medicine, Institute of Liver and Biliary Sciences, D1 Vasant Kunj Road, New Delhi, Delhi 110070, India
E-mail: savykaur@gmail.com

Key words: hepatocellular carcinoma, endothelial cells, cancer stem cells, angiogenesis

VEGF on several tumorigenic properties of hepatoma cell lines were investigated in the present study.

Materials and methods

Cells and cell culture. Human liver hepatoma Huh7 (p53mut) and liver cancer HepG2 (p53^{+/+}) cell lines were obtained from the National Centre for Cell Science (Pune, India). All cell lines were cultured in Dulbecco's modified Eagle's medium (DMEM; Gibco; Thermo Fisher Scientific, Inc.) with 10% FBS (HyClone; Cytiva) and 100 $\mu\text{g/ml}$ streptomycin and 100 IU/ml penicillin (Gibco; Thermo Fisher Scientific, Inc.) at 37°C in incubator containing 5% CO₂. Human umbilical vein endothelial cells (HUVECs), which are primary cell line (cat. no. CL019; Hi-media Laboratories, LLC) were grown in endothelial medium (HiMedia Laboratories, LLC) with growth factors and 1% antibiotics (100 $\mu\text{g/ml}$ streptomycin and 100 IU/ml penicillin) on gelatin-coated plates.

Co-culture of cells. In order to examine the mechanisms through which endothelial cells modulate the tumorigenic behaviour of HBx-transfected hepatoma cells, direct and indirect co-cultures were performed. For indirect co-cultures, Huh7 cells were treated with conditioned medium (CM) from HUVECs. CMs were prepared after serum starvation of these cells for 24 h and then collecting the supernatants after centrifugation to remove cell debris. For obtaining VEGF-induced cells, hepatoma cells were exposed to a 10 ng/ml VEGF concentration for 48 h (17).

Drug induction in cells. For the evaluation of the effects of the inhibition of VEGF on hepatoma cells, the cells were exposed to a sorafenib (BAY-BAYERS Corporation) at a concentration of 15 μM , dissolved in 0.1% dimethyl sulfoxide (DMSO, HiMedia Laboratories, LLC) for 24 h (18).

Cell proliferation. Initially, Huh7 cells were seeded at a concentration of 30,000 cells/well in a 6-well plate and incubated overnight at 37°C. On the following day, the cells were exposed to VEGF and incubated for 24 h at 37°C. Following 24 h, the cells were trypsinized, stained with trypan blue (HiMedia Laboratories, LLC) at room temperature and immediately counted using a haemocytometer chamber slide. Cell numbers were counted manually at 10X objective using under an inverted light microscope (NIKON Eclipse Ti inverted microscope, Nikon Corporation), and the average of three independent experiments was used.

Transwell assays. Control and VEGF-induced hepatoma cells were detached, harvested by centrifugation (75 g for 5 min at 25°C) and resuspended in DMEM (without serum), and then 50,000 cells per chamber placed in the upper chamber of a modified Boyden chamber consisting of uncoated polycarbonate filter membranes of an 8- μm pore size. For invasion, the Transwell insert was first coated with Matrigel. The chamber was placed in a 24-well culture dish containing DMEM with FBS in the lower chamber. After 24 h (for chemotaxis) and 48 h (for invasion) incubation at 37°C, the lower side of the filter was washed with PBS and fixed with 4% paraformaldehyde (HiMedia Laboratories, LLC) for 2 min at room temperature.

The cells were then washed and permeabilized by 100% methanol (HiMedia Laboratories, LLC) for 20 min at room temperature. For quantification, cell nuclei were stained with 0.5% crystal violet (HiMedia Laboratories, LLC) for 15 min at RT. The upper side of the filter containing the non-migrating cells was scraped with a cotton swab. Cells migrating towards the lower chamber were counted manually at 4X objective in random fields under an inverted light microscope (NIKON Eclipse Ti inverted microscope, Nikon Corporation).

Wound healing assay. Control, VEGF-induced and sorafenib-treated hepatoma cells were plated in 12-well plates (3x10⁶ cells/well). Following a 6-h exposure to serum-starved conditions, a scratch was made on the cell layer using a 100 μl sterile micropipette tip, in order to create a wound. The cells were photographed using a phase-contrast microscope (NIKON Eclipse Ti inverted microscope, Nikon Corporation), to determine the wound width at the 0 h time point. Following a 24-h culture, the cells were photographed again. Wound healing was visualized by comparing cell layers at 0 h with those at 24 h, analysing the distance migrated by the leading edge of the wound at each time point in all the study groups. The relative wound width was measured as wound width at the 24-h timepoint, divided by the wound width at the 0-h time point. Measurements were made using Software NIS Elements (version 2.3) of the NIKON Eclipse Ti inverted microscope (Nikon Corporation). The width was measured in μm .

Tube formation assay. Huh7 cells were seeded at 50,000 cells/well with HUVECs at a 1:1 ratio for direct co-culture on a growth factor-reduced Matrigel-coated 24-well plate and were incubated overnight at 37°C. For indirect co-cultures, hepatoma cells were seeded at 50,000 cells/well with CM from HUVECs including VEGF (10 ng/ μl) on Matrigel, as described above. The average number (from 4-5 fields) of tube networks and circles per field were counted manually, under an inverted microscope (NIKON Eclipse Ti inverted microscope, Nikon Corporation) and photographed at 10X objective.

Reverse transcription-quantitative PCR (RT-qPCR) analysis. Control, VEGF-induced and sorafenib-treated hepatoma cells were harvested using trypsin-EDTA solution (0.25%). Total RNA was isolated by using Trizol[®] reagent (Thermo Fisher Scientific, Inc.) and quantified at 260/280 nm using a Thermo Scientific Nanodrop 2000 Spectrophotometer (Thermo Fisher Scientific, Inc.). The absorption ratio A260/A280 nm between 1.90 and 2 was considered to indicate adequate RNA quality. First strand cDNA was synthesized from 1 μg of total RNA using reverse transcriptase (cat. no# AB1453B; Verso cDNA synthesis kit; Thermo Fisher Scientific, Inc.) according to the manufacturer instructions. qPCR was performed by using SYBR-Green PCR master mix (Fermentas; Thermo Fisher Scientific, Inc.) on the ViiA7 instrument PCR system (Applied Biosystems; Thermo Fisher Scientific, Inc.). The following cycling parameters were used: Start at 95°C for 5 min, denaturing at 95°C for 30 sec, annealing at 60°C for 30 sec, elongation at 72°C for 30 sec, and a final 5 min extra extension at the end of the reaction and repeated for 40 amplification

cycles. The primer pairs used in the present study are listed in Table SI.

3D spheroid cultures. Tumour spheroids were generated by seeding 4,000 cells/well in six-well ultra-low attachment culture plates (Corning Inc.), culturing them in DMEM/F12 (Gibco; Thermo Fisher Scientific, Inc.) supplemented with 5% FBS (HyClone; Cytiva) then incubated at 37°C in a 5% CO₂ incubator for 2-3 days; after 3 days the medium was replaced with serum-free medium (with or without VEGF; 10 ng/μl). For HUVEC direct co-culture spheroids, Huh7 and HUVECs were grown at a 1:1 ratio with DMEM plus endothelial medium at a ratio of 1:1 and for indirect co-cultures, the medium was replaced with CM of HUVECs. Spheroids were further grown on ultra-low attachment plates for 2 weeks in order to establish 3D anchorage-independent models. The 3D anchorage-independent models were imaged using a Nikon Eclipse Ti inverted microscope (Nikon Corporation) and the average size of the spheroids was measured using ImageJ Software (version 2.3, National Institutes of Health).

Hanging drop cultures. The hanging drop method was utilized to evaluate the tumorigenic potential of HCC tumour spheroids. Untreated and treated cells (with VEGF, 10 ng/μl and/or sorafenib, 15 μM) were seeded in a hanging-drop plate at a concentration of 1,000 cells/μl in growth medium. Images of drops were obtained at 24 and 72 h post-treatment. Tumour spheroid adhesion occurrence was scored on a 0-2 scale, with '0' score depicting no spheroid formation, '1' the formation of a loose spheroid, and '2' signifying compact spheroid formation. Migration was visualized by comparing the 0-h with the 24- and 72-h images and analyzing the distance migrated by the cells to aggregate at each time point in all the study groups. Relative migration percentage was measured as the migrated cell area at 24 and 72 h, divided by the total area covered by seeded cells at 0-h time point. All measurements were performed using Software NIS Elements (version 2.3) from NIKON Eclipse Ti (Nikon Corporation). In order to obtain morphometric data, two to three individual plates of each condition were imaged, and four to six images were obtained from each plate. Calibrated images were exported using ImageJ software, (version, 1.53e, National Institutes of Health) for morphometric analysis. The polygon tool was used to outline the spheroids and projected area was measured as $[4\pi \times (\text{area})]/(\text{perimeter})^2$. The measurement unit was μm (19-21).

Spheroid invasion assay. Spheroids (1-week-old; both VEGF-induced and control) were seeded in 24-well cell culture plates on which the Matrigel (5 mg/ml) was coated (Life technologies; Thermo Fisher Scientific, Inc.). Images were obtained at various time points (days 2, 5, 7 and 10) at 20x magnification using an inverted microscope (Nikon Ti Eclipse; Nikon Corporation). Area invaded by the cells was evaluated by assessing the sprouting areas per spheroid which were quantified using ImageJ software (version 1.53e) (13,19,22).

Immunofluorescence and histological analysis. Spheroids were fixed in 4% paraformaldehyde (HiMedia Laboratories, LLC) over night at 4°C. Subsequently, the spheroids were

rinsed with PBS (HiMedia Laboratories, LLC) and stained with 0.1% eosin (HiMedia Laboratories, LLC) for 15 min at room temperature. For cryosectioning, the spheroids were embedded in cryostat freezing mix (Sakura Finetek, USA) at -20°C. Sections of 4 μm thickness were mounted on pre-warmed slides. Standard haematoxylin- and eosin spheroid-stained slides (staining at room temperature for 8 and 5 min, respectively) were first evaluated to confirm spheroid quality. For immunofluorescence staining, 4-μm-thick cryosections were cut and hydrated with 0.5% BSA-PBS (HiMedia) for 15 min. The sections were exposed to blocking buffer (0.1% donkey serum-PBS; Sigma-Aldrich; Merck KGaA) for 30 min. The spheroids were then incubated overnight using primary mouse Vimentin (VIM) antibody (1:50, Cat no# sc-6260; Santa Cruz Biotechnology, Inc.; 1:50) at 4°C. After washing, cells were incubated with anti-mouse Alexa Fluor 594 (Dilution 1:500, Cat no#sc-516608, Santa Cruz Biotechnology, Inc.) secondary antibody for 45 min at RT. Finally, the sections were mounted with DAPI (HiMedia) for 5 min at RT. Stained images were acquired using a fluorescent microscope (Nikon Ti Eclipse; Nikon Corporation). For 2D culture immunofluorescence, Huh7 cells were first permeabilized with Triton-X (0.1%, HiMedia) and followed by 4% paraformaldehyde. Following this, cells were blocked with serum (1% FBS (Hyclone) in PBS (HiMedia) for 1 h. All remaining staining protocol steps were performed as previously described. Number of fluorescent cells were counted manually (n=3) using ImageJ software (version 1.53e, National Institutes of Health) by applying a 'sharp edges cell filter' and the percentage was calculated according to the ratio of average number of VIM-positive cells to the average number of DAPI-stained cells per field (in 2D culture).

Cell adhesion assay. Briefly, 48-well plates pre-coated with fibronectin (10 ng/ul; FN, Himedia) and bovine serum albumin (1% BSA; both HiMedia) were washed with PBS twice and blocked for 1 h at 37°C with DMEM (Gibco; Thermo Fisher Scientific, Inc.) containing 0.1% BSA (HiMedia) before plating the cells. A cell suspension containing 2x10⁵ cells/ml (control and VEGF-induced Huh7 cells) was prepared in serum-free medium. The cell suspension (150 μl) was added to each well (BSA-coated wells acting as a negative control). Cells were allowed to adhere for 1 h at 37°C. Subsequently, the unadhered cells were removed by gentle washing three times with PBS. Adherent cells were stained with 0.5% crystal violet for 10 min at room temperature and the optical density values were measured at 405 nm wavelength using microplate reader (Synergy/H1 Hybrid Multimode Plate Reader; Agilent Technologies, Inc.).

MTT assay. For the assay, 10,000 cells/well were plated [control, VEGF-induced and sorafenib (15 μM) treated Huh7 cells] in a 96-well plate and incubated at 24 and 48 h. Cells were washed with PBS and 20 μl MTT (0.5 mg/ml; HiMedia) were added to each well of the plate. The plates were incubated at 37°C for 4 h. Subsequently, 200 μl DMSO was added for formazan solubilization and mixed thoroughly and left in the dark for 10 min. Intensity of the colour developed was recorded at 570 nm using a fluorescence microplate reader (Synergy/H1 Hybrid Multimode Plate Reader; Agilent Technologies, Inc.).

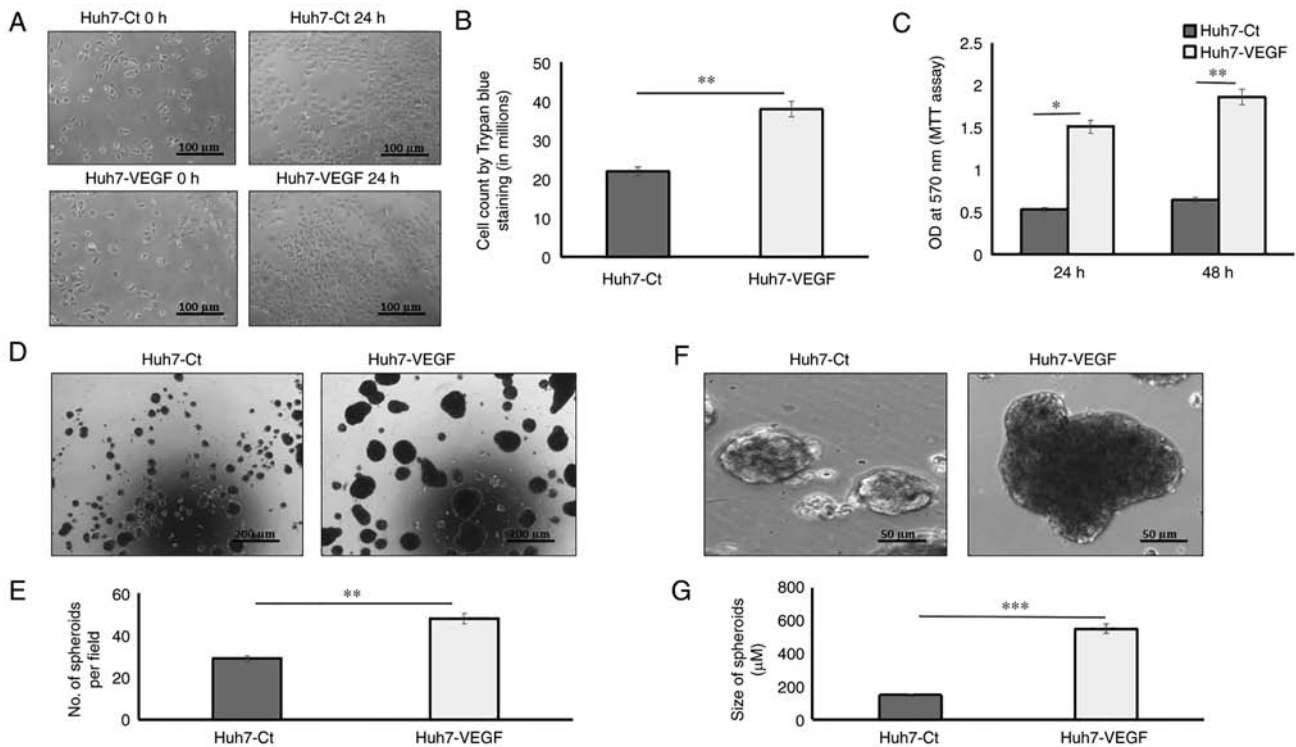


Figure 1. Proliferation assay and tumor growth assay in 2D and 3D culture respectively. (A and B) Phase contrast images of Huh7 cells (treated with VEGF and media alone; magnification, x10) and bar chart demonstrating the number of cells proliferated per well using trypan blue dye exclusion assay (number in millions). (C) Bar chart, depicting MTT assay; OD at 570 nm in Huh7 (control), Huh7 cells induced with VEGF at 24 and 48 h time points. (D and E) Phase contrast images of the number of spheroids formed by Huh7 cells (treated with VEGF and media alone) per field (magnification, x4) and bar chart, demonstrating spheroid number per field. (F and G) Phase contrast images of size of spheroids formed by Huh7 cells (treated with VEGF and medium alone) per field (magnification, x20) and bar chart demonstrating the size of spheroids per field (in μm). Data are represented as the mean \pm SD. (n=3 each). * $P < 0.05$, ** $P < 0.01$ and *** $P < 0.001$. VEGF, vascular endothelial growth factor.

Statistical analysis. All quantitative data are expressed as the mean \pm standard deviation.

An unpaired Student's t-test was used for analyses and comparisons between two groups. For multiple group analyses and comparisons, one-way ANOVA was used, with the subsequent application of Tukey's post hoc test. All experiments were repeated at least three times. $P < 0.05$ was considered to indicate a statistically significant difference.

Results

VEGF promotes tumour growth in 2D and 3D cultures. To examine the effects of VEGF on tumour growth, the hepatoma cells were incubated with VEGF in 2D and 3D tumour cell models. In 2D models, cell proliferation was assessed by counting the actual number of cells using trypan blue exclusion experiments and also using MTT cell viability assay. Following a 24-h incubation with VEGF, the cell numbers were found to be significantly higher in the VEGF-induced Huh7 cells as compared to the control Huh7 cells (Fig. 1A and B; $P < 0.05$). MTT assay also revealed that VEGF induction enhanced the proliferation of Huh7 cells both after 24 h ($P < 0.05$) and 48 h ($P < 0.01$) as compared to the control Huh7 cells (Fig. 1C). In 3D models, tumour growth was assessed using spheroid growth in ultra-low attachment plates as suspension cultures, for 2 weeks, continuously, to avoid sub-culturing. Huh7 cells (4,000 cells/well) without or with VEGF induction formed distinct spheroids within 14 days of suspension

culture (Fig. 1D and F). The number of spheroids and their sizes revealed that the VEGF-induced Huh7 spheroids were significantly increased in number (Fig. 1E; $P < 0.01$) and also larger in size (551 μm ; 3.7-fold), as compared to the spheroids formed by hepatoma cells without VEGF induction (146 μm ; Fig. 1G; $P < 0.001$).

Tumorigenic properties in the presence of VEGF in 2D vs. 3D cultures. In 2D hepatoma models, the wound healing, adhesion and migration potential of the hepatoma cells were examined, in order to investigate the tumorigenic properties. The results depicted that VEGF-induced Huh7 cells exhibited a relatively smaller wound width or increased migration (Fig. 2A and B; $P < 0.01$), increased adhesion (Fig. 2C) and higher chemotaxis (Fig. 2D and E; $P < 0.05$), as compared to the control Huh7 cells. In 3D models, non-adherent hanging drop cultures for spheroid formation were used to evaluate the tumorigenic property, on which cellular aggregation is promoted based on gravity and there is complete absence of a substratum. The adhesion property by the formation of 3D spheroids was evaluated within a stringent time point i.e., on days 0 to 3, and the adhesion of cells to form spheroids and the spheroid compactness was considered as a measure of tumorigenic property. On day 3, cell-to-cell adhesion and spheroid compaction were significantly increased in spheroids which were treated with VEGF, as compared to spheroids derived from control cells in the absence of VEGF (Fig. 2F and G; $P < 0.01$). Migration was assessed by the distance covered by cells within a confined space to form a spheroid from

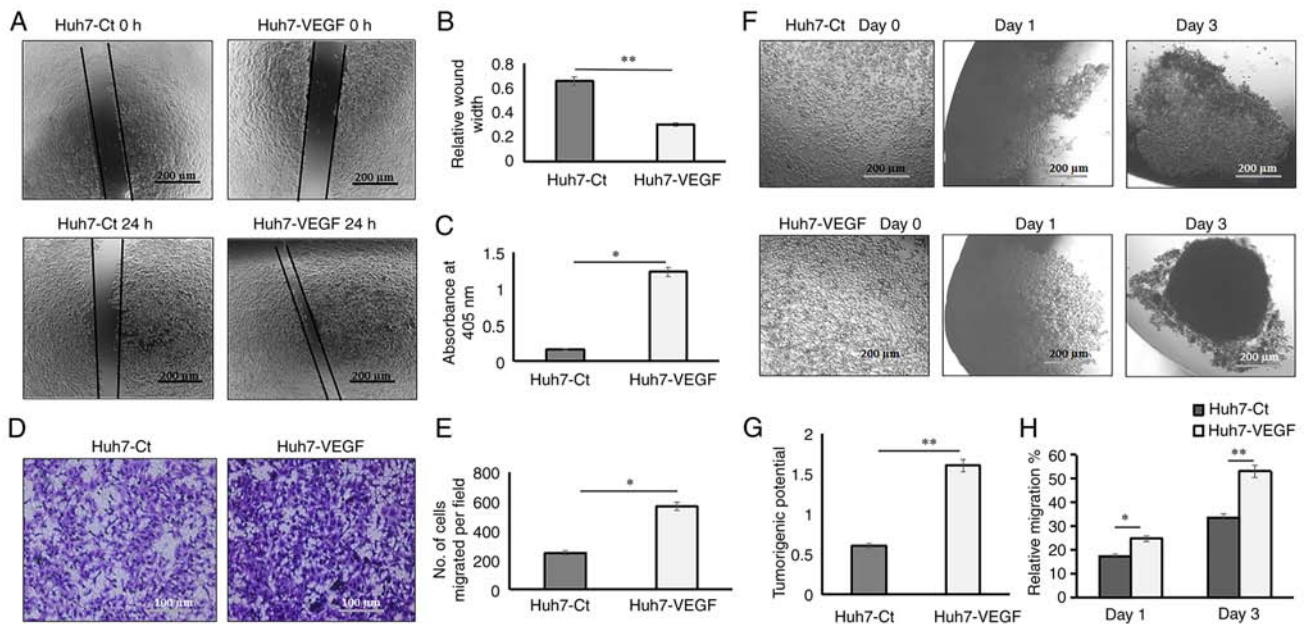


Figure 2. Migration assays in 2D and 3D co-cultures. (A) Phase contrast images of wound healing scratch assay demonstrating the migration of cells after the creation of a scratch in Huh7 cells with VEGF-induced and control conditions at 0 and 24 h (magnification, x4). (B) Bar chart demonstrating the average of relative wound width at 24 h divided by the 0-h wound width under various conditions. (C) Bar chart demonstrating the adhesion of cells on fibronectin coating; the absorbance was measured at 405 nm. (D) Phase contrast images of Transwell assays, demonstrating the migration of Huh7 cells (control and VEGF-induced) from the upper chamber towards the lower chamber after 24 h; magnification, x10. (E) Bar chart demonstrating the number of migrated control and VEGF-induced cells in Transwell assays. (F) Phase contrast images of Huh7 spheroid formation in the control and VEGF treated cells at the day 1 and 3 time points, to evaluate tumorigenic potential of cells (magnification, x4). (G) Bar chart demonstrating the tumorigenic potential of control and VEGF-Huh7 cells. (H) Bar chart demonstrating the relative migration percentage of control and VEGF-Huh7 cells. The average size of the spheroids is presented in Table SII. Data are presented as the mean \pm SD (n=3 each). *P<0.05 and **P<0.01. VEGF, vascular endothelial growth factor; Ct, control.

days 0 to days 1 and 3. The results revealed that on day 3, the percentage of migrating cells in the hanging drop able to form a compact spheroid was 53.10% in the VEGF-induced cells as compared to 33.64% in the control cells (Fig. 2H; P<0.01). The average spheroid sizes are presented in Table SII.

Invasive properties in the presence of VEGF in 2D vs. 3D cultures. Tumour invasion in 2D cultures was measured as number of cells invading through the extracellular matrix (ECM; Matrigel-coated Transwell) per field, and the invasion in 3D models was measured as the average percentage of area invaded by the spheroids (n=4) through the ECM (Matrigel). In 2D models, the results demonstrated that the numbers of Huh7 cells that invaded through the Matrigel were increased when incubated with VEGF, as compared to the control Huh7 cells after 48 h (Fig. 3A and B; P<0.05). In 3D models, the VEGF-induced spheroids that invaded into the Matrigel (which functioned as ECM) after day 2, demonstrated an enhanced invasive potential at various time points, namely day 2 (Fig. 3D), day 5 (Fig. 3E; P<0.05), day 7 (Fig. 3F; P<0.05) and day 10 (Fig. 3G; P<0.01). The results also revealed that after day 10, the VEGF-induced spheroids formed some vessel-like structures (black arrows, Fig. 3C) inside the Matrigel. The average spheroid sizes are presented in Table SII.

VEGF enhances the stemness potential and triggers EMT in the 2D monolayer and 3D spheroid model. In 2D models, gene expression data revealed an upregulation of mesenchymal genes, including VIM (Fig. 4B; P<0.05), N-cadherin [or Cadherin 2 (CDH2); Fig. S1A; P<0.01], Thy-1 cell surface antigen

(THY-1; Fig. S1B; P<0.05) and the cancer stemness marker, CD133 (Fig. 4C; P<0.05), while E-cadherin [or Cadherin 1 (CDH1); epithelial marker; Fig. 4A] in VEGF-induced Huh7 cells was downregulated in comparison to the control cells. CDH1 gene expression data were also validated in the HepG2 liver cancer cell line. The results revealed the upregulation of the mesenchymal genes, VIM (Fig. S2B; P<0.05), CDH2 (Fig. S2D), THY-1 (Fig. S2E; P<0.01), and the cancer stemness marker, CD133 (Fig. S2C; P<0.01), while CDH1 (Fig. S2A) in the VEGF-induced HepG2 cells was downregulated in comparison to the control HepG2 cells in 2D cultures. In 3D models, gene expression analysis demonstrated an upregulation in the expression of the mesenchymal genes, VIM (Fig. 4F; P<0.05), CDH2 (Fig. S3A, P<0.05), THY-1 (Fig. S3B; P<0.01) and CD133 (Fig. 4G; P<0.01), while the expression of CDH1 in the spheroids was only slightly reduced in presence of VEGF (Fig. 4E). In 2D culture models, the results of immunofluorescence staining revealed the increased expression of the mesenchymal marker, VIM (1.49-fold higher, Fig. S4A and B; P<0.01) in the VEGF-induced Huh7 cells as compared to the control cells (Fig. 4D). In 3D spheroid cultures, haematoxylin and eosin staining revealed better integrity and homogenous cell morphology in VEGF-induced spheroids, as compared to the control spheroids (Fig. 4H). There was no marked difference in the expression of the mesenchymal protein, VIM in the 3D spheroids treated with and without VEGF (Fig. 4H).

Tumor growth in 2D and 3D cultures of hepatoma cells co-cultured with endothelial cells. In order to determine the mechanisms through which heterogenous cell cultures

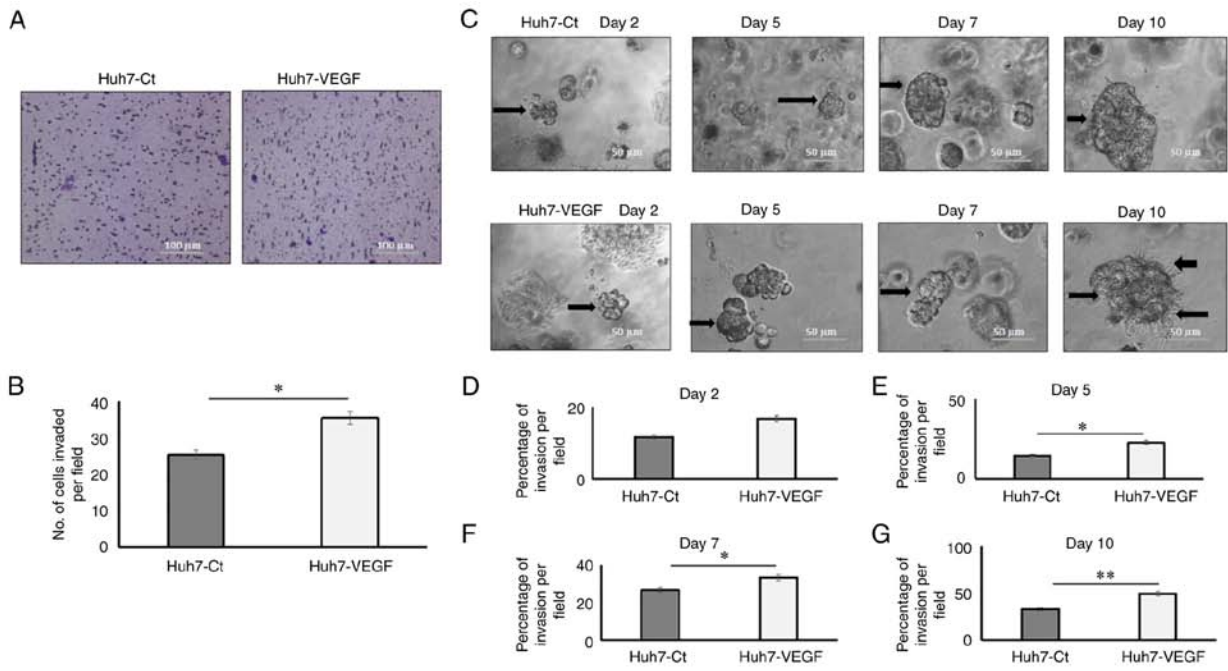


Figure 3. Invasion assay in 2D and 3D co-cultures. (A) Phase contrast images of Transwell assays, demonstrating the invasion of Huh7 cells (control and VEGF-induced from the upper chamber toward lower chamber after 24 h; magnification, x10). (B) Bar chart demonstrating the number of invaded control and VEGF-induced cells in Transwell assays. (C) Phase contrast images of invasion of control and VEGF-induced Huh7 cells spheroids inside the Matrigel at various time points (days 2, 5, 7 and 10; magnification, x20). (D-G) Bar charts presenting the percentage of invasion in the control and VEGF-spheroids at various time points (days 2, 5, 7 and 10). The average size of the spheroids is presented in Table SII. Data are presented as the mean \pm SD (n=3 each). *P<0.05 and **P<0.01. VEGF, vascular endothelial growth factor.

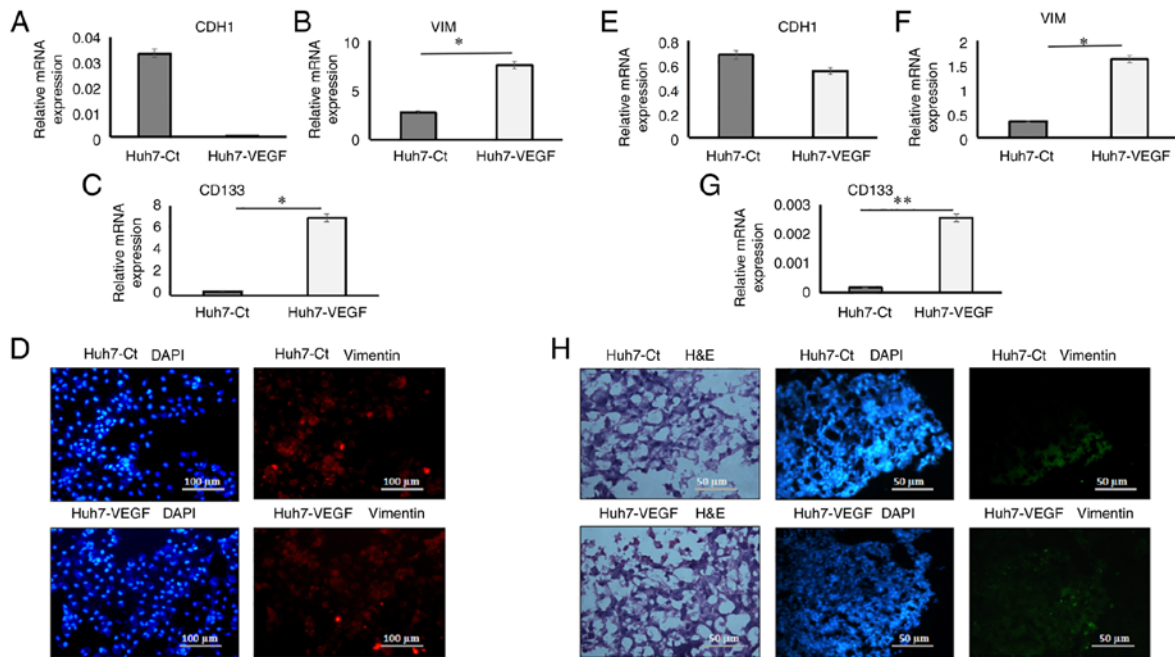


Figure 4. Epithelial-mesenchymal transition and cancer stemness gene expression and mesenchymal protein expression in 2D and 3D co-cultures. Relative mRNA expression of (A) CDH1 (B) VIM (C) CD133 in Huh7 cells in presence of control medium and VEGF in 2D models (D) Staining of mesenchymal protein, VIM and DAPI in control and VEGF-induced Huh7 cells (magnification, x10). Relative mRNA expression of (E) CDH1 (F) VIM (G) CD133 in Huh7 cells in presence of control medium and VEGF in 3D models. (H) H&E images of control and VEGF-induced spheroid (magnification, x20) and staining of mesenchymal protein, VIM and DAPI in control and VEGF-induced spheroid (magnification, x20). Data are presented as the mean \pm SD (n=3 each). *P<0.05 and **P<0.01. VIM, vimentin; Ct, control; VEGF, vascular endothelial growth factor; CDH1, cadherin 1 (E-cadherin); H&E, haematoxylin and eosin.

functioned in 2D and 3D hepatoma models, HUVECs and Huh7 cells were concurrently cultured in direct and indirect cultures on Matrigel-coated wells. In 2D cultures,

the results depicted that branch points (Fig. 5A and B; P<0.0001) and tube lengths (Fig. 5A and C; P<0.05) were significantly enhanced when Huh7 cells were co-cultured

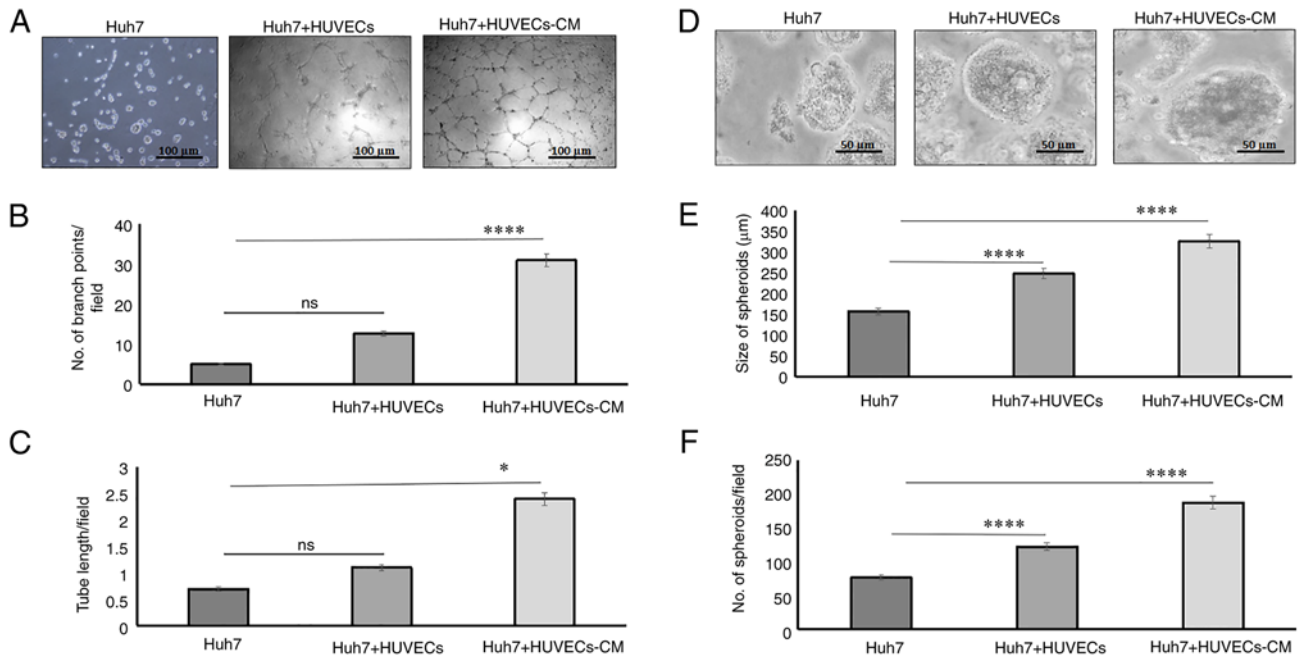


Figure 5. Matrigel tube assay in co-cultures. (A) Phase contrast images of Huh7 cells alone, co-cultures of Huh7:HUVECs (1:1) and Huh7 + HUVECs-CM on Matrigel (magnification, x10). (B) Bar chart demonstrating the number of average network circles per field formed on the Matrigel under various conditions. (C) Bar chart demonstrating the average tube length per field formed on the Matrigel under various conditions. (D) Phase contrast images of the size of spheroids formed by Huh7 cells alone and Huh7 in co-cultures (Huh7 + HUVECs and Huh7 + HUVECs-CM) per field (magnification, x20) and (E and F) Bar charts demonstrating the size (in μm) and number of spheroids per field, respectively. ANOVA, followed by the Tukey's multiple comparison post hoc test, was used for multiple group data analysis. Data are presented as the mean \pm SD (n=3 each). * $P<0.05$ and **** $P<0.0001$. HUVECs, human umbilical venules endothelial cells; CM, condition medium.

with HUVEC-CM, as compared to single-Huh7 cultures (Fig. 5A-C). In direct 2D cultures, where Huh7 cells were cultured with HUVECs at a 1:1 ratio, the tubes were not well-formed on the Matrigel (Fig. 5A-C). Hence, we next developed anchorage-independent heterologous 3D models of Huh7 cells and HUVECs. Size and number of the spheroids was significantly increased in Huh7 cells cultured with HUVECs (n=122; $P<0.0001$, 248.184 μm ; 1.5-fold; $P<0.0001$) or when Huh7 cells were co-cultured with HUVEC-CM (n=187; $P<0.0001$, 325.631 μm ; 2-fold; $P<0.0001$), as compared to single Huh7 cultures (n=76; $P<0.0001$, 157.846 μm ; Fig. 5D-F).

Sorafenib, a multikinase inhibitor reduces migratory properties in VEGF-induced 2D and 3D cultures. The cytotoxicity of sorafenib on Huh7 cells in the absence or presence of VEGF was determined using MTT assay. It was demonstrated that the viability of VEGF-untreated and VEGF-treated Huh7 cells was reduced by 19.8 and 29% respectively, following treatment with sorafenib for 24 h (Fig. S5; $P<0.01$). The effect of sorafenib on the 2D hepatoma cell culture migratory ability was evaluated by wound healing assay. In 2D and 3D cultures, in the presence of VEGF, sorafenib treatment resulted in a considerable reduction in migration in 2D cultures; i.e., a decreased wound healing ability as compared with untreated cells (Fig. 6A and B; $P<0.05$). In 3D cultures, on day 3, cell to cell adhesion and spheroid compaction were significantly decreased in the sorafenib-treated spheroids as compared to the spheroids derived from control cells in presence of VEGF (Fig. 6C and D, $P<0.05$). In addition, on day 3, the percentage of migration and compact spheroid formation

was reduced in the hanging drops by sorafenib-treated cells as compared to that observed in the control cells (50.77 vs. 65.82%; $P<0.01$, Fig. 6E). The average size of spheroids is presented in Table SII. Furthermore, the effect of the angiogenesis inhibitor, sorafenib, on the expression of EMT-related genes in 2D and 3D VEGF-induced hepatoma models was analysed. In 2D models, the gene expression data revealed the upregulated expression levels of mesenchymal VIM (Fig. S6B) and CDH2 (Fig. S6C, $P<0.05$) and cancer stemness marker, CD133 (Fig. S6D), whereas there was no significant difference in the expression of CDH1 (epithelial marker; Fig. S6A) in the sorafenib-treated cells, in comparison with the control cells. In the 3D models, sorafenib treatment resulted in downregulation in the expression of the mesenchymal genes, VIM (Fig. S6B; $P<0.01$), CDH2 (Fig. S6C; $P<0.01$) and CD133 (Fig. S6D; $P<0.01$), while the differences in CDH1 expression in spheroids were not statistically significant between groups in the absence or presence of sorafenib (Fig. S6A).

In the context of migration, there was a 0.46-fold inhibition in 2D models while in 3D models, the inhibition in cell migration was 1.29-fold (Fig. 6A-E). Similarly, in terms of mesenchymal gene expression, in the 3D models, VIM expression was reduced by 2.27-fold in sorafenib-treated cells as compared to that observed in untreated cells, while in 2D models, VIM expression was decreased only by 1.23-fold in sorafenib-treated cells as compared to that in untreated cells (Fig. S6B). Expression of the cancer stemness gene, CD133 was also reduced by 2.25-fold in the 3D models, while in 2D models, it decreased only by 1.03-fold (Fig. S6D, in comparison with untreated cells in respective conditions).

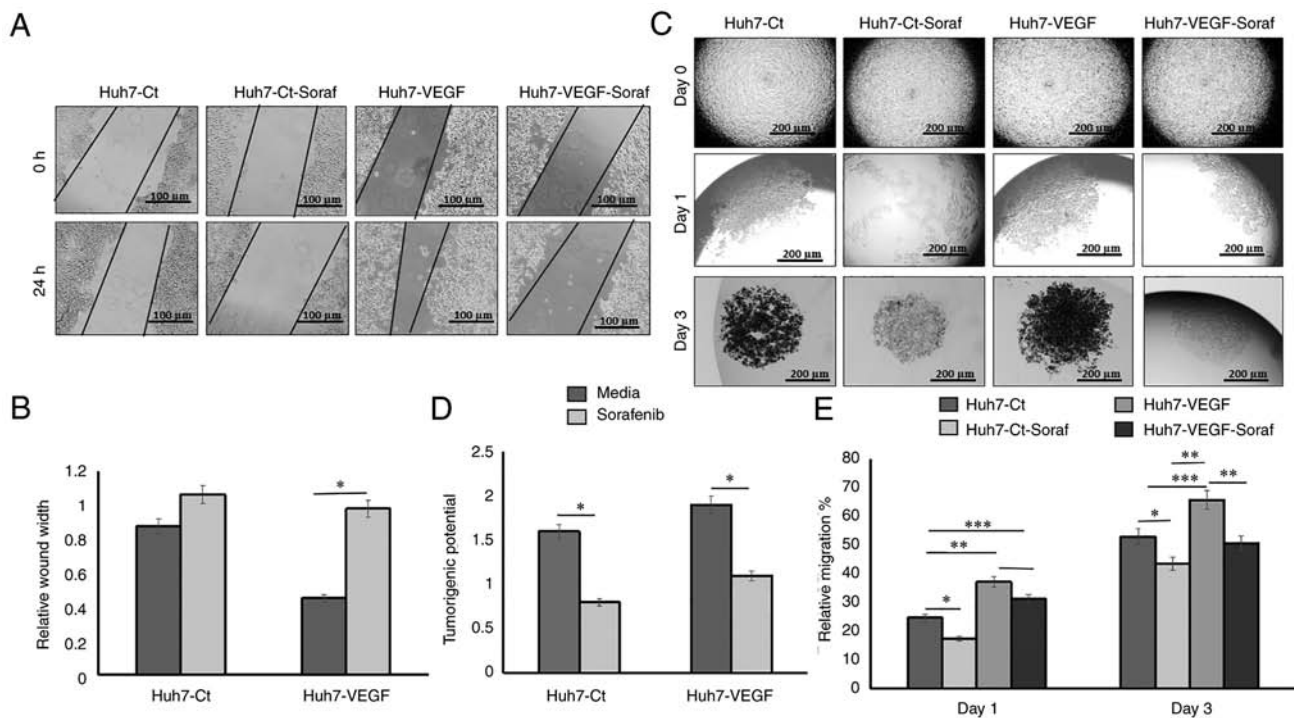


Figure 6. Migration in 2D and 3D co-cultures after sorafenib treatment. (A) Phase contrast images of wound healing scratch assay demonstrating the migration of cells after the creation of a scratch in Huh7 cells with sorafenib-induced and control conditions at 0 and 24 h (magnification, x10) in VEGF-treated and untreated cells. (B) Bar chart demonstrating the average of relative wound width at 24 h width divided by the 0-h wound width under various conditions. (C) Phase contrast images of Huh7 spheroid formation in control and sorafenib-induced cells on the day 1 and 3 time points, to evaluate tumorigenic potential of VEGF-treated and untreated cells (magnification, x4). (D) Bar chart demonstrating the tumorigenic potential and (E) relative migration percentage of cells in the various groups. Tukey's multiple comparisons test in ANOVA was used for multiple group data analysis. The average size of spheroids is presented in Table SII. Data are presented as the mean \pm SD ($n=3$ each). * $P<0.05$, ** $P<0.01$ and *** $P<0.001$. VEGF, vascular endothelial growth factor.

Discussion

In the present study, the role of VEGF in inducing EMT and cancer stemness in both 2D and 3D models of HCC was investigated. In 2D models, the only known measure for tumour growth and invasion is the increase in cell numbers, whereas in anchorage-independent 3D spheroid models, the estimation of spheroid sizes may also reflect *in vivo* aspects of tumour growth (23). Hepatoma cells cultured in anchorage-independent 3D models have been demonstrated to exhibit increased stemness and gene expression in previous studies. Jung *et al* (24) previously reported Huh7 hanging drop models and Khawar *et al* (25) used Huh7 liquid overlay cultures for 3D tumour-related studies, in which tumour cells aggregate spontaneously, without an exogenous supply of ECM. These spheroids are heterogeneous cell populations (e.g., hypoxic vs. normoxic, quiescent vs. replicating cells), have a well-defined geometry and undergo optimal physiological cell-to-cell interactions (26-28). In 3D models, hepatoma cells formed well-defined spheroids (551 μm in diameter) in the presence of VEGF in a time period of 2 weeks. In hanging drop cultures, cells migrated towards each other, ultimately aggregating in the drop, and then formed a compact spheroid which was a result of cell-to-cell adhesion (20). Hence, the migration and adhesion of hepatoma cells in these spheroids, considered as a measure of tumorigenic property, were considerably enhanced in cell cultures treated with VEGF, similar to that reported in a previous study utilizing 2D cell culture models (29). 3D model is an improved model for the study of tumorigenic properties,

since both migration and adhesion can be studied in a single experimental model. By contrast, in the 2D monolayer model, two sets of experiments are required to study both characteristics. The invasive properties of HCC models were studied in presence of Matrigel, in 2D and 3D formats. The presence of Matrigel, which represents the ECM, adds another level of complexity to the 2D vs. 3D differences. Matrigel invasion assays demonstrated that hepatoma cells were capable of invading efficiently in the presence of VEGF in comparison to cells in the control media. In 3D models, it was feasible to efficiently monitor spheroid invasion in different days, whereas invasion in 2D models could be recorded only after 48 h. Similar to 3D models, it was attempted to study tumour invasion on different days for 2D models; however, the results were not consistent, possibly as only the number of cells invading through the ECM matrix (Matrigel) were counted, as a parameter for the evaluation of invasion. In 3D models, sprouting in the spheroids treated with VEGF after the 10th day was also observed, indicating that 3D spheroids may be a promising model to simultaneously study invasion and angiogenesis. However, angiogenesis was not extensively studied on Matrigel in the 3D models, since a significant formation of tubes and capillaries in 3D conditions, requires media provision to the spheroids by using a perfusion/fluidic system, which was not applied in the present study. HCC is a fairly unique type of carcinoma, in which fibrosis and chronic inflammation precedes the development of HCC in >90% of cases (30). An excessive deposition of the ECM has been reported as a key hallmark of HCC (31). Hence, studying the

tumorigenic potential and invasiveness of hepatoma cells in presence of ECM substrates, such as Matrigel is relevant (25).

The present study then investigated whether the 3D tumour spheroids also exhibit a gene expression profile, characterized by EMT and stemness. In our previous study, we demonstrated that TGF- β imparted mesenchymal traits to the hepatoma cells (32). In another study, Takai *et al* (33) cultured different hepatoma cells on varied matrices, demonstrating that cells in porous alginate scaffolds may be able to generate organoid-like spheroids that mimic numerous *in vivo* features. It was stated in their study that EpCAM⁺ hepatoma cells cultured as spheroids may be more sensitive to TGF β -induced EMT and possess increased tumorigenic and metastatic potential, as compared to conventional 2D cultures. The variability of TGF β -mediated tumorigenic effects on 2D and 3D cultures have also been reported in ovarian cell lines (34). In the present study, the effects of VEGF on the tumour properties of hepatoma cells were evaluated in a 2D, as well as in a 3D microenvironment. The results revealed that hepatoma cells formed 3D spheroids, which differed in size and density in absence and presence of the same VEGF concentration. In all spheroids, tumour invasion and angiogenesis were more aggressive in 3D cultures in comparison to 2D conditions, following treatment with VEGF. In terms of gene expression, the VEGF-mediated increase in the levels of the EMT markers, VIM, CDH2 and THY-1 was observed in both 2D and 3D cultures; however, the increase was more notable in the 2D conditions as compared to that observed in 3D conditions, which may be attributed to the fact that tumour cells in 3D conditions may be differentially exposed to VEGF. CDH1, a cell-to-cell adhesion receptor is an important determinant of tumour progression and it has been reported to be downregulated in numerous HCC tumours (35). In the presence of VEGF, no change in CDH1 gene expression was observed in 3D models, whereas in 2D models, a decreased expression of CDH1 was observed, which was in line with a previously published study (36). Of note, a proportionate increase in the remaining gene expression levels was not observed in the 3D models, in comparison to the 2D models. These findings suggested that 3D cultures potentially avoid the overestimation of mechanistic observations in 2D cultures, which may be ascribed to many reasons. Firstly, cells in 2D are all at the same cell cycle stage, whereas 3D cells are often in different cell cycle stages resembling to cells *in vivo*, due to oxygen and nutrient gradients. 3D models have limited media permeability, which may have an impact on cell viability and gene expression. Secondly, spheroid cells at the leading edge are metabolically active and show the greatest invasive and proliferative capacities. By contrast, the cells that are located away from this leading edge, towards the tumour centre have been reported to be more quiescent and less proliferative (37). Furthermore, spheroids often present in uneven sizes, with several areas including great numbers of growing tumour cells, and other areas including reduced tumour cell numbers. Thus, it may be difficult to acquire a 3D culture with all spheroids having identical features, particularly when they are grown without a substratum. Hence, at a given time, the number and type of cells exposed to an exogenous factor may vary in different wells, which may have resulted in heterogeneous gene expression values. By contrast, under 2D adherent cell culture conditions, cell lines derived from all three stages

appeared phenotypically alike and presented with similar motility characteristics. This may possibly be the main reason for gene expression heterogeneity in 3D cultures, as compared to 2D cultures. However, since this similar scenario also exists *in vivo*, it is pertinent that the results obtained in 2D models should be cautiously extrapolated to *in vivo* models in future studies.

To further validate the role of VEGF in inducing the tumorigenic properties of hepatoma cells, 2D and 3D culture studies were also performed using the VEGFR-inhibitor, sorafenib (at a recommended concentration of 15 μ M), in VEGF-treated Huh7 cells for 24 h. Sorafenib has been suggested to inhibit hepatoma growth in the presence of hypoxia and hypoxia-induced angiogenesis (38). A parallelism in the efficacy of sorafenib in well-differentiated cells cultured in both 3D and 2D models was described in another study (39). Cheng *et al* (40) reported that combined treatment with sorafenib and dasatinib (another kinase inhibitor) effectively inhibited HCC cell-induced angiogenesis. In particular, they demonstrated that the administration of a regular 10 μ M-dose of sorafenib in both 3D and 2D cultures may be effective at reducing cell proliferation and a reduction in the spheroid area in both Huh7 and HepG2 cell lines (40). In accordance with these findings, in the present study, sorafenib treatment culminated in a marked reduction in cell migration in both 2D and 3D cultures and of spheroid size in 3D cultures. However, a higher reduction of cell migratory properties and a decrease in the expression of mesenchymal genes was observed in 3D cultures, as compared to the 2D cultures, following sorafenib treatment, indicating that 3D cultures may serve as a more promising and reliable model for screening the effectiveness of tumour-inhibiting therapeutics. The use of 2D and 3D models was also analysed to study the interactions between HUVECs and hepatoma cells in both direct (with HUVECs) and indirect cultures (with HUVEC-CM). HUVECs have been previously reported to promote EMT (41). VEGF and angiogenin secreted by the HUVECs have also been reported to induce proliferation and invasion of hepatoma cells (24). Hence, both direct and indirect cultures (both 2D and 3D) of HUVECs with hepatoma cells were used to examine the mechanisms through which HUVECs may affect tumour invasion. In 2D monolayer conditions, although indirect cultures of hepatoma cells in the presence of HUVEC-CM revealed an increase in tube-like structures, direct cultures of hepatoma cells with HUVECs did not demonstrate significant changes in branch point numbers, as well as the tube length of cells, in comparison to that observed in single hepatoma cell culture. In 3D spheroid culture models, the number of spheroids was significantly increased in both direct and indirect cultures, as compared to HUVECs alone, possibly suggesting that 2D monolayer models are not suitable to study organotypic/heterogenous cell tumour cell models, with 3D models being more reliable and predictive. In the present study, Huh7 cell lines were used to examine the effects of VEGF after VEGF induction, in 2D and 3D cultures. HepG2 cell lines have not been previously used, to the best of our knowledge, in 3D cultures, but only in several 2D culture-related studies. Fukuyama *et al* (42) stated in their study that three liver cancer cell lines (Huh7, HepG2 and Hep3B) fell in the same hierarchical cluster and shared a common origin. These cell lines and primary hepatocytes

appeared next to each other in cluster and demonstrated similar gene expression patterns. However, due to various gene mutations, several genetic and growth heterogeneities in different hepatic cell lines have been reported (43). Hence, the use of additional liver cancer cell lines, including HepG2 and Hep3B, is required to determine whether the effects of VEGF on 3D conditions are cell-specific.

The observations of the present study suggested that the effects of growth factors as predicted in 2D cultures may markedly differ than those in 3D cultures and hence, in the *in vivo* setting. Taken together, the present study indicated subtle differences between the 2D and 3D culture systems, in terms of invasive phenotype and EMT-associated gene expression profile of hepatoma cells in the presence of VEGF.

In conclusion, the present study demonstrated that the tumorigenic properties of invasion and migration in response to growth factors and/or therapeutics can be most effectively studied in 3D setting as compared to the 2D setting. Additionally, gene expression changes obtained in 2D cultures in response to different treatment regimens require careful interpretations. Numerous anti-tumour therapeutics appearing to be promising in a 2D cell culture setup, fail heavily during clinical studies. A better understanding of HCC with patient-specific cells in 3D cultures *in vitro* models would certainly provide an improved comprehension of HCC biology *in vivo*, the prediction of the response of hepatoma cells to targeted therapy, as well as the development of novel therapeutic concepts.

Acknowledgements

Not applicable.

Funding

The present study was supported by the DBT-RGYI grant (BT/PR6356/GBD/27/407/2012).

Availability of data and materials

The datasets used and/or analysed during the current study are available from the corresponding author on reasonable request.

Authors' contributions

PR performed cell culture experiments, migration, chemotaxis, invasion, immunophenotyping, RT-qPCR and 3D culture assays, collected and analysed data and drafted the manuscript. DMT designed the experiments. VN analysed data. SK designed the study and performed data analysis. All authors have read and approved the final manuscript. PR and SK confirm the authenticity of all the raw data.

Ethics approval and consent to participate

Not applicable.

Patient consent for publication

Not applicable.

Competing interests

The authors declare that they have no competing interests.

References

- Forner A, Reig M and Bruix J: Hepatocellular carcinoma. *Lancet* 391: 1301-1314, 2018.
- Zhang Y, Gao X, Zhu Y, Kadel D, Sun H, Chen J, Luo Q, Sun H, Yang L, Yang J, *et al*: The dual blockade of MET and VEGFR2 signaling demonstrates pronounced inhibition on tumor growth and metastasis of hepatocellular carcinoma. *J Exp Clin Cancer Res* 37: 93, 2018.
- Ma S, Pradeep S, Hu W, Zhang D, Coleman R and Sood A: The role of tumor microenvironment in resistance to anti-angiogenic therapy. *F1000Res* 7: 326, 2018.
- Jiang Z, Zhai X, Shi B, Luo D and Jin B: KIAA1199 overexpression is associated with abnormal expression of EMT markers and is a novel independent prognostic biomarker for hepatocellular carcinoma. *Onco Targets Ther* 11: 8341-8348, 2018.
- Li L and Li W: Epithelial-mesenchymal transition in human cancer: Comprehensive reprogramming of metabolism, epigenetics, and differentiation. *Pharmacol Ther* 150: 33-46, 2015.
- Silvestre JS, Lévy BI and Tedgui A: Mechanisms of angiogenesis and remodelling of the microvasculature. *Cardiovasc Res* 78: 201-202, 2008.
- Zhao W, Zhao T, Huang V, Chen Y, Ahokas RA and Sun Y: Platelet-derived growth factor involvement in myocardial remodeling following infarction. *J Mol Cell Cardiol* 51: 830-838, 2011.
- Crivellato E, Nico B, Vacca A, Djonov V, Presta M and Ribatti D: Recombinant human erythropoietin induces intussusceptive microvascular growth *in vivo*. *Leukemia* 18: 331-336, 2004.
- Zhan X, Wang F, Bi Y and Ji B: Animal models of gastrointestinal and liver diseases. Animal models of acute and chronic pancreatitis. *Am J Physiol Gastrointest Liver Physiol* 311: G343-G355, 2016.
- Liu S, Sun Y, Jiang M, Li Y, Tian Y, Xue W, Ding N, Sun Y, Cheng C, Li J, *et al*: Glyceraldehyde-3-phosphate dehydrogenase promotes liver tumorigenesis by modulating phosphoglycerate dehydrogenase. *Hepatology* 66: 631-645, 2017.
- Karunakaran D, Rashmi R and Kumar TR: Induction of apoptosis by curcumin and its implications for cancer therapy. *Curr Cancer Drug Targets* 5: 117-129, 2005.
- Fantozzi A, Gruber DC, Pisarsky L, Heck C, Kunita A, Yilmaz M, Meyer-Schaller N, Cornille K, Hopfer U, Bentires-Alj M and Cristofori G: VEGF-mediated angiogenesis links EMT-induced cancer stemness to tumor initiation. *Cancer Res* 74: 1566-1575, 2014.
- Takai A, Dang H, Oishi N, Khatib S, Martin SP, Dominguez DA, Luo J, Bagni R, Wu X, Powell K, *et al*: Genome-wide RNAi screen identifies PMPCB as a therapeutic vulnerability in EpCAM⁺ hepatocellular carcinoma. *Cancer Res* 79: 2379-2391, 2019.
- Kozyra M, Johansson I, Nordling Å, Ullah S, Lauschke VM and Ingelman-Sundberg M: Human hepatic 3D spheroids as a model for steatosis and insulin resistance. *Sci Rep* 8: 14297, 2018.
- Loessner D, Rizzi SC, Stok KS, Fuehrmann T, Hollier B, Magdolen V, Hutmacher DW and Clements JA: A bioengineered 3D ovarian cancer model for the assessment of peptidase-mediated enhancement of spheroid growth and intraperitoneal spread. *Biomaterials* 34: 7389-7400, 2013.
- Pingitore P and Romeo S: The role of PNPLA3 in health and disease. *Biochim Biophys Acta Mol Cell Biol Lipids* 1864: 900-906, 2019.
- Sarkanen JR, Kaila V, Mannerström B, Rätty S, Kuokkanen H, Miettinen S and Ylikomi T: Human adipose tissue extract induces angiogenesis and adipogenesis *in vitro*. *Tissue Eng Part A* 18: 17-25, 2012.
- Chiang IT, Liu YC, Wang WH, Hsu FT, Chen HW, Lin WJ, Chang WY and Hwang JJ: Sorafenib inhibits TPA-induced MMP-9 and VEGF expression via suppression of ERK/NF-κB pathway in hepatocellular carcinoma cells. *In Vivo* 26: 671-681, 2012.
- Bell CC, Hendriks DF, Moro SM, Ellis E, Walsh J, Renblom A, Fredriksson Puigvert L, Dankers AC, Jacobs F, Snoeyens J, *et al*: Characterization of primary human hepatocyte spheroids as a model system for drug-induced liver injury, liver function and disease. *Sci Rep* 6: 25187, 2016.

20. Raghavan S, Mehta P, Horst EN, Ward MR, Rowley KR and Mehta G: Comparative analysis of tumor spheroid generation techniques for differential in vitro drug toxicity. *Oncotarget* 7: 16948-16961, 2016.
21. Murad HY, Bortz EP, Yu H, Luo D, Halliburton GM, Sholl AB and Khismatullin DB: Phenotypic alterations in liver cancer cells induced by mechanochemical disruption. *Sci Rep* 9: 19538, 2019.
22. D'Angelo E, Natarajan D, Sensi F, Ajayi O, Fassan M, Mammano E, Pilati P, Pavan P, Bresolin S, Preziosi M, *et al*: Patient-derived scaffolds of colorectal cancer metastases as an organotypic 3D model of the liver metastatic microenvironment. *Cancers (Basel)* 12: 364, 2020.
23. Kapałczyńska M, Kolenda T, Przybyła W, Zajączkowska M, Teresiak A, Filas V, Ibbs M, Bliźniak R, Łuczewski Ł and Lamperska K: 2D and 3D cell cultures—a comparison of different types of cancer cell cultures. *Arch Med Sci* 14: 910-919, 2018.
24. Jung HR, Kang HM, Ryu JW, Kim DS, Noh KH, Kim ES, Lee HJ, Chung KS, Cho HS, Kim NS, *et al*: Cell spheroids with enhanced aggressiveness to mimic human liver cancer in vitro and in vivo. *Sci Rep* 7: 10499, 2017.
25. Khawar IA, Park JK, Jung ES, Lee MA, Chang S and Kuh HJ: Three dimensional mixed-cell spheroids mimic stroma-mediated chemoresistance and invasive migration in hepatocellular carcinoma. *Neoplasia* 20: 800-812, 2018.
26. Hirschhaeuser F, Menne H, Dittfeld C, West J, Mueller-Klieser W and Kunz-Schughart LA: Multicellular tumor spheroids: An underestimated tool is catching up again. *J Biotechnol* 148: 3-15, 2010.
27. Kunz-Schughart LA, Freyer JP, Hofstaedter F and Ebner R: The use of 3-D cultures for high-throughput screening: The multicellular spheroid model. *J Biomol Screen* 9: 273-285, 2004.
28. Lin RZ and Chang HY: Recent advances in three-dimensional multicellular spheroid culture for biomedical research. *Biotechnol J* 3: 1172-1184, 2008.
29. Bhattacharya R, Fan F, Wang R, Ye X, Xia L, Boulbes D and Ellis LM: Intracrine VEGF signalling mediates colorectal cancer cell migration and invasion. *Br J Cancer* 117: 848-855, 2017.
30. Refolo MG, Messa C, Guerra V, Carr BI and D'Alessandro R: Inflammatory mechanisms of HCC development. *Cancers (Basel)* 12: 641, 2020.
31. Muenzner JK, Kunze P, Lindner P, Polaschek S, Menke K, Eckstein M, Geppert CI, Chanvorachote P, Baeuerle T, Hartmann A and Schneider-Stock R: Generation and characterization of hepatocellular carcinoma cell lines with enhanced cancer stem cell potential. *J Cell Mol Med* 22: 6238-6248, 2018.
32. Rawal P, Siddiqui H, Hassan M, Choudhary MC, Tripathi DM, Nain V, Trehanpati N and Kaur S: Endothelial cell-derived TGF- β promotes epithelial-mesenchymal transition via CD133 in HBx-infected hepatoma cells. *Front Oncol* 9: 308, 2019.
33. Takai A, Fako V, Dang H, Forgues M, Yu Z, Budhu A and Wang XW: Three-dimensional organotypic culture models of human hepatocellular carcinoma. *Sci Rep* 6: 21174, 2016.
34. Al Ameri W, Ahmed I, Al-Dasim FM, Ali Mohamoud Y, Al-Azwani IK, Malek JA and Karedath T: Cell Type-specific TGF- β mediated EMT in 3D and 2D models and its reversal by TGF- β receptor kinase inhibitor in ovarian cancer cell lines. *Int J Mol Sci* 20: 3568, 2019.
35. Schneider MR, Hiltwein F, Grill J, Blum H, Krebs S, Klanner A, Bauersachs S, Bruns C, Longrich T, Horst D, *et al*: Evidence for a role of E-cadherin in suppressing liver carcinogenesis in mice and men. *Carcinogenesis* 35: 1855-1862, 2014.
36. Melissaridou S, Wiechec E, Magan M, Jain MV, Chung MK, Farnebo L and Roberg K: The effect of 2D and 3D cell cultures on treatment response, EMT profile and stem cell features in head and neck cancer. *Cancer Cell Int* 19: 16, 2019.
37. Smalley KS, Lioni M, Noma K, Haass NK and Herlyn M: In vitro three-dimensional tumor microenvironment models for anticancer drug discovery. *Expert Opin Drug Discov* 3: 1-10, 2008.
38. Li F, Wang F and Wu J: Sorafenib inhibits growth of hepatoma with hypoxia and hypoxia-driven angiogenesis in nude mice. *Neoplasma* 64: 718-724, 2017.
39. Rodríguez-Hernández MA, Chapresto-Garzón R, Cadenas M, Navarro-Villarán E, Negrete M, Gómez-Bravo MA, Victor VM, Padillo FJ and Muntané J: Differential effectiveness of tyrosine kinase inhibitors in 2D/3D culture according to cell differentiation, p53 status and mitochondrial respiration in liver cancer cells. *Csell Death Dis* 11: 339, 2020.
40. Cheng CC, Chao WT, Shih JH, Lai YS, Hsu YH and Liu YH: Sorafenib combined with dasatinib therapy inhibits cell viability, migration, and angiogenesis synergistically in hepatocellular carcinoma. *Cancer Chemother Pharmacol* 88: 143-153, 2021.
41. Ou J, Guan D and Yang Y: Non-contact co-culture with human vascular endothelial cells promotes epithelial-to-mesenchymal transition of cervical cancer SiHa cells by activating the NOTCH1/LOX/SNAIL pathway. *Cell Mol Biol Lett* 24: 39, 2019.
42. Fukuyama K, Asagiri M, Sugimoto M, Tsushima H, Seo S, Taura K, Uemoto S and Iwaisako K: Gene expression profiles of liver cancer cell lines reveal two hepatocyte-like and fibroblast-like clusters. *PLoS One* 16: e0245939, 2021.
43. Zhao Y, Chen Y, Hu Y, Wang J, Xie X, He G, Chen H, Shao Q, Zeng H and Zhang H: Genomic alterations across six hepatocellular carcinoma cell lines by panel-based sequencing. *Transl Cancer Res* 7: 231-239, 2018.



This work is licensed under a Creative Commons Attribution-NonCommercial-NoDerivatives 4.0 International (CC BY-NC-ND 4.0) License.